# A study of the structure and chiral selectivity of micelles of two isomeric D-glucopyranoside-based surfactants

**David Tickle,[a] Ashley George,[b] Kevin Jennings,[b] Patrick Camilleri *,[b] and Anthony J. Kirby[a]**

[a] *University Chemical Laboratory, Lensfield Road, Cambridge, UK CB2 1EW*
[b] *SmithKline Beecham Pharmaceuticals, New Frontiers Science Park, Coldharbour Road, The Pinnacles, Harlow, Essex, UK CM19 5AD*

**We have synthesised the sodium salts of two isomeric surfactants that differ in the anomeric orientation of the $C_{14}$ hydrocarbon chain to the D-glucopyranoside fused ring structure, containing a phosphate polar head group. The inclusion of α- and β-anomers in the separation buffer, using micellar electrokinetic capillary chromatography (MECC) shows that the latter is the superior chiral selector. The critical micelle concentration (cmc) for both surfactants was around 0.6 mM, and the mean aggregation number is 65 for both anomers. In an attempt to understand the possible mechanism of chiral discrimination, we have calculated minimum energy conformations of micelles produced by these surfactants, and have established the importance of their chiral head groups and the sodium counter-ions in the discriminating process. We have also investigated the micro-structures of the two surfactants by transmission electron microscopy. This technique shows that the two enantiomers aggregate very differently; whereas the α-anomer shows randomly orientated string-like forms the β-anomer forms ordered 'whorl' arrays.**

Major advances in the synthesis and commercial production of single enantiomers as biologically active molecules require the development of selective and sensitive analytical methods, suitable for the analysis of one enantiomer in the presence of a vast excess of the other. Until recently traditional 'wet' separation techniques, in particular thin layer chromatography (TLC) and high performance liquid chromatography (HPLC) have been the methods of choice for the analysis of enantiomeric species. The high separation efficiencies routinely achieved in capillary electrophoresis (CE) have enhanced its popularity for the resolution of mixtures of enantiomers related to molecules that vary widely in their structure, lipophilicity and ionisation. This technique is becoming increasingly effective in monitoring enantiomeric purity of both intermediates and final drug product.

In this application of CE, chiral additives are added to the separation buffer, and the mode of operation is usually free zone electrophoresis or micellar electrokinetic capillary chromatography (MECC). Chiral selectors have included naturally occurring additives such as cyclodextrins,[1–3] bile salts,[4,5] proteins[6] and peptide antibiotics.[7] We have also reported the design and synthesis of anionic surfactants, which when used above their critical micelle concentration (cmc) in MECC allow the resolution of a number of structurally unrelated racemic mixtures.[8–10] The formation of non-covalent 'diastereoisomers' between the micelles and the enantiomers leads to chiral discrimination if the energies of formation of these transient species differ sufficiently.

Of the various structures of chiral surfactants we have so far synthesised for chiral CE discrimination, glucopyranoside-based surfactants[8] have been the most successful. To obtain information about the mechanism of chiral resolution by this class of anionic detergents we have now prepared the two isomeric molecules, **1** and **2** that differ in the anomeric orientation of the hydrocarbon chain with respect to the glucopyranoside ring.

Differences in the chiral discrimination properties of micelles formed from the sodium salts of the α- and β-anomers have been observed in the MECC analysis of a number of amino acid dansyl derivatives. In an attempt to account for variations in chiral selectivity by these surfactants we have measured their respective aggregation and critical micelle concentration (cmc) values. We also report studies on the microstructures of the two surfactants by molecular modelling and transmission electron microscopy.

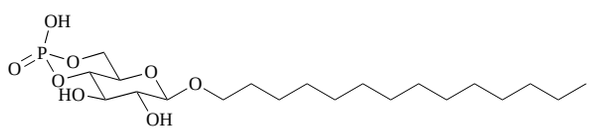

**1,** β-anomer

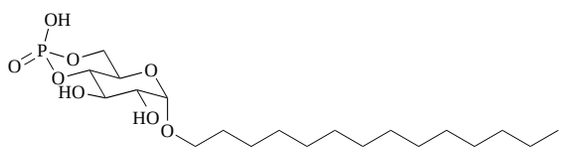

**2,** α-anomer

## Experimental

### Materials

Starting materials and reagents for the synthesis of surfactants **1** and **2** and intermediates were purchased from Aldrich (Gillingham, Dorset, UK). Dansyl derivatives and buffer constituents for capillary electrophoresis and phosphotungstic acid for electron transmission microscopy were purchased from Agar Scientific (Stanstead, UK). Tris(2,2′-bipyridyl)ruthenium chloride, 9-methylanthracene and *N*-phenyl-1-naphthylamine were obtained from ICN Biomedicals Ltd. (High Wycombe, Bucks, UK). Solutions were prepared in doubly-distilled water throughout.

### Synthesis of the sodium salt of *n*-tetradecyl β-D-glucopyranoside 4,6-(hydrogen phosphate) 1

**Tetradecyl 2,3,4,6-tetra-*O*-acetyl-β-D-glucopyranoside 3.** Acetobromoglucose (9.4 g, 0.23 mmol) was added to a stirred solution containing *n*-tetradecanol (6.9 g, 0.32 mmol), yellow

mercuric oxide (7.1 g, 32 mmol), mercuric bromide (0.2 g, 0.7 mmol) and Drierite (10 g) in 100 $cm^3$ of dry dichloromethane and the solution stirred at room temp. for 20 h under argon. The mixture was then filtered, the solids washed with dichloromethane, and the filtrate combined with the washings, then washed with 1 M KBr (4 × 50 $cm^3$) until no mercuric salts were present in the washings. The organic layer was then washed with water, dried ($Na_2SO_4$) and concentrated *in vacuo*. The residue was purified by repeated column chromatography [$SiO_2$, light petroleum (bp 30–40 °C)–EtOAc; 2:1] to yield the tetraacetyl glucopyranoside **3** (4.2 g, 34%) as needles, mp 57–59 °C; $R_f$ [$SiO_2$, light petroleum (bp 30–40 °C)–EtOAc; 2:1], 0.58; $\nu_{max}/cm^{-1}$ ($CH_2Cl_2$) 1757 (C=O) and 1262 (CO); $\delta_H$(400 MHz; $CDCl_3$; *J* values in Hz throughout) 5.17 (1 H, t, *J* 9.5, CHOAc), 5.05 (1 H, t, *J* 9.7, CHOAc), 4.95 (1 H, dd, *J* 9.5 and 8.1, CHOAc), 4.45 (1 H, d, *J* 8.0, OCHO), 4.23 (1 H, dd, *J* 12.3 and 4.3, C$H_A$$H_B$OAc), 4.09 (1 H, dd, *J* 12.3 and 2.1, CH$_A$-$H_B$OAc), 3.83 (1 H, dt, *J* 9.5 and 6.3, OC$H_A$$H_B$R), 3.66 (1 H, ddd, *J* 9.9, 4.4 and 2.3, CHO), 3.43 (1 H, dt, *J* 9.5 and 6.9, OCH$_A$$H_B$R), 2.05 (3 H, s, $CH_3$), 2.00 (3 H, s, $CH_3$), 1.98 (3 H, s, $CH_3$), 1.97 (3 H, s, $CH_3$), 1.55–1.48 (2 H, m, $OCH_2CH_2C_{12}H_{25}$), 1.27–1.20 (22 H, m, $OC_2H_4C_{11}H_{22}CH_3$) and 0.84 (3 H, t, *J* 6.7, $CH_3$); $\delta_C$(62.5 MHz, $CDCl_3$) † 170.7−, 170.3−, 169.4−, 169.3− (4 × CO), 108.8+ (OCHO), 72.9+, 71.7+, 71.3+ (3 × CHOAc), 70.2− ($OCH_2R$), 68.5+ (CHO), 62.0+ ($CH_2OAc$), 31.9−, 29.7−, 29.6−, 29.6−, 29.4−, 29.4−, 29.3−, 29.3−, 25.8−, 25.8−, 22.7−, 20.7+, 20.6+ and 14.1+; *m*/*z* (EI) 424.3 (10%, $M^+ - 2 \times OAc$), 351.2 (10%, $M^+ - C_{14}H_{29}$), 331.1 (50%, $M^+ - OC_{14}H_{29}$), 55.0 (100%, $C_4H_7$) (Found: $M^+ - C_4H_6O_4$ 424.2834, $C_{24}H_{40}O_6$ requires 424.2825).

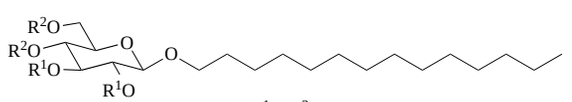


**3** $R^1 = R^2 = Ac$
**4** $R^1 = R^2 = H$
**5** $R^1 = H$, $R^2R^2 =$ 


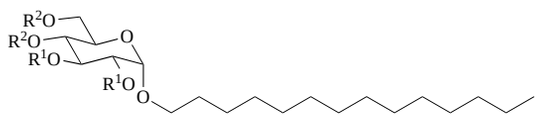


**6** $R^1 = R^2 = H$
**7** $R^1 = H$, $R^2R^2 =$ 


**Tetradecyl β-D-glucopyranoside 4.** A solution of sodium methoxide in methanol (1 M; 20 $cm^3$) was added to a stirred solution of tetraacetyl glucopyranoside **3** (4.2 g, 11.2 mmol) in 50 $cm^3$ of dry methanol. The resulting solution was stirred for 2 h under argon. It was then desalted by the addition of ~30 g of Dowex 50 W ($H^+$) resin and stirred overnight. The solution was then filtered and the residual resin washed with methanol. The washings were combined with the filtrate and the residue was purified by flash column chromatography ($SiO_2$, $CH_2Cl_2$–MeOH, 9:1) to give the glycoside **4** (2.9 g, 99.8%) as needles, mp 119–121 °C; $R_f$ ($SiO_2$, $CH_2Cl_2$–MeOH, 9:1), 0.2; $\nu_{max}/cm^{-1}$ ($CH_2Cl_2$) 3410 (OH) and 1078 (CO); $\delta_H$[400 MHz, $(CD_3)_2SO$] 4.94 [1 H, d, *J* 5.0, CHO*H* (exc.)], 4.92 [1 H, d, *J* 5.41, CHO*H* (exc.)], 4.90 [1 H, d, *J* 4.6, CHO*H* (exc.)], 4.47 [1 H, t, *J* 5.9, $CH_2OH$ (exc.)], 4.08 (1 H, d, *J* 7.8, OCHO), 3.74 (1 H, dt, *J* 9.4 and 6.9, OC$H_A$$H_B$R), 3.65 (1 H, dd, *J* 11.5 and 5.9, C$H_A$$H_B$OH), 3.5–3.35 (2 H, m, OCH$_A$$H_B$R and CH$_A$$H_B$-OH), 3.2–3.0 (3 H, m, 2 × C*H*OH and CHO), 2.91 (1 H, td, *J* 7.9 and 5.0, C*H*OH), 1.5–1.45 (2 H, m, $OCH_2CH_2R$), 1.3–1.2 (22 H, m, $OC_2H_4C_{11}H_{22}CH_3$) and 0.85 (3 H, t, *J* 6.7); $\delta_C$[100 MHz, $(CD_3)_2SO$] 102.9+ (OCHO), 76.9+, 73.5+, 70.2+, 68.6− ($OCH_2R$), 61.2− ($CH_2OH$), 31.4−, 29.4−, 29.2−, 29.1−, 28.9−, 25.7−, 22.2− and 14.04+; *m*/*z* (EI) 376.3 (0.5%, $M^+$), 345.3 (20%, $M^+ - CH_2OH$), 197.2 (60%, $OC_{12}H_{25}$), 73.0 (100%, $C_4H_8O$) (Found: $M^+$, 376.2824, $C_{20}H_{40}O_6$ requires 376.2824).

**Tetradecyl β-D-glucopyranoside 4,6-(phenyl phosphate) 5.** Dry triethylamine (0.8 $cm^3$, 9.1 mmol) was added to a stirred solution of glycopyranoside **4** (2.49 g, 6.6 mmol) in 500 $cm^3$ of dry dichloromethane containing 5 g of 4 Å molecular sieves and the solution was stirred under argon for 1 h. The solution was then cooled to 0 °C, phenyldichlorophosphate (1.4 g, 6.6 mmol) added and the reaction stirred for another 3 h at room temp. The solution was then filtered and the filtrate concentrated *in vacuo*. The residue was purified by flash column chromatography ($SiO_2$, EtOAc–hexane, 1:1) to yield the two diastereoisomers (4:1) of the phosphate triester **5** (1.76 g, 51.7%) as a clear oil; $R_f$ ($SiO_2$, EtOAc–hexane, 1:1), 0.1; $\nu_{max}/cm^{-1}$ ($CH_2Cl_2$) 3584 (OH), 1592, 1490 (C=C), 1316 (P=O) and 1205 (PO); $\delta_H$(400 MHz, $CDCl_3$) (major isomer) 7.40–7.10 (5 H, m, Ph), 4.50–4.35 (1 H, m, C$H_A$$H_B$OP), 4.42 (1 H, d, *J* 7.8, OCHO), 4.27 (1 H, t, *J* 10.4, CHOP), 4.18 (1 H, t, *J* 9.4, C*H*OH), 3.90–3.65 (3 H, m, CH$_A$$H_B$OP, OC$H_A$$H_B$R and CHO), 3.53 (1 H, dt, *J* 9.2 and 7.0, OCH$_A$$H_B$R), 3.43 (1 H, t, *J* 8.5, C*H*OH), 1.60–1.50 (2 H, m, $OCH_2CH_2R$), 1.30–1.20 (22 H, m, $OC_2H_4C_{11}H_{22}CH_3$), 0.86 (3 H, t, *J* 6.8, $CH_3$); (no additional signals due to minor isomers); $\delta_C$(100 MHz, $CDCl_3$) (major isomer) 150.0− ($C_{ipso}$), 130.1+ ($C_{meta}$), 125.6+ ($C_{para}$), 119.6+ (1 C, d, *J* 4.9, $C_{ortho}$), 80.6+ (1 C, d, *J* 6.6, CHOP), 73.7+ (CHOH), 73.3+ (1 C, d, *J* 8.5, CHOH), 70.8− ($OCH_2R$), 69.0− (1 C, d, *J* 7.8, $CH_2OP$), 66.0 (1 C, d, *J* 5.7, CHO), 31.9−, 29.7−, 29.6−, 29.6−, 29.4−, 29.4−, 25.9−, 22.7− and 14.2+; (additional signals due to minor isomer) 129.9+ ($C_{meta}$), 125.8+ ($C_{para}$), 120.3+ (1 C, d, *J* 4.5, $C_{ortho}$), 103.2+ (OCHO), 79.4+ (CHOP), 73.9+ (CHOH), 73.5+ (CHOH), 70.7− ($OCH_2R$), 68.6− ($CH_2OP$) and 66.2+ (CHO); *m*/*z* (FAB) 515.5 (8%, $MH^+$), 175 (100%, $PhOPO_3H_2$) (Found: $MH^+$, 1 515.278 50. $C_{26}H_{44}O_8$ requires 515.2774).

**Tetradecyl β-D-glucopyranoside 4,6-(hydrogen phosphate), sodium salt 1.** Aqueous sodium hydroxide (1 M; 5 $cm^3$) was added to a stirred solution of phosphate triester **5** (1.67 g, 3.2 mmol) in 45 $cm^3$ THF and the solution stirred for 15 h. The solution was concentrated *in vacuo* to approximately 10 $cm^3$ and neutralized with 1 M HCl. The resulting solution was then lyophilized to yield a white powder which was placed in a Soxhlet extractor and washed with dichloromethane for 48 h to yield the phosphate diester **1** (1.40 g, 93.6%) as white flakes; $\nu_{max}/cm^{-1}$ (Nujol) 3580 (OH), 1320 (P=O); $\delta_H$(400 MHz, $D_2O$) 4.44 (1 H, d, *J* 7.2, OCHO), 4.2–4.0 (1 H, m, CHOP), 3.93 (1 H, t, *J* 9.1, C*H*OH), 3.9–3.2 (6 H, m, $CH_2OP$, CHO, C*H*OH and $OCH_2R$), 1.7–1.6 (2 H, m, $OCH_2CH_2R$), 1.4–1.2 (22 H, m, $OC_2H_4C_{11}H_{22}CH_3$) and 0.83 (3 H, t, *J* 6.0, $CH_3$); $\delta_C$(100 MHz, $D_2O$) 106.1+ (OCHO), 80.4+ (CHOP), 76.2+, 75.8+ (2 × CHOH), 73.2− ($OCH_2R$), 70.0+ (CHO), 69.2− ($CH_2OP$), 34.7−, 32.8−, 32.7−, 32.3−, 32.2−, 28.6−, 25.4− and 16.5+; $\delta_P$(250 MHz, $D_2O$, H-decoupled) −142.9; $\delta_P$(250 MHz, $D_2O$, H-coupled) −142.9 (1 P, d, *J* 57.8); *m*/*z* (−ve FAB) 437 [5%, $(M - Na^+)^-$], 551 [100%, $(M - Na^+ + TFA)^-$].

### Synthesis of the sodium salt of *n*-tetradecyl α-D glucopyranoside 4,6-(hydrogen phosphate) 2

**Tetradecyl α-D-glucopyranoside 6.** *n*-Tetradecanol (0.8 g, 3.8 mmol) was added to a stirred solution of the tetraacetyl glycoside **3** (2.08 g, 3.8 mmol), in 20 $cm^3$ of dry dichloromethane under argon. 1 M tin(IV) chloride in dichloromethane (3.8 $cm^3$, 3.8 mmol) was added dropwise and the resulting solution was stirred for 48 h. The solution was then diluted with dichloromethane (100 $cm^3$), washed with 3 M HCl (2 × 50 $cm^3$), dried ($MgSO_4$) and concentrated *in vacuo*. Crude NMR of the residue showed a product ratio of greater than 95:5 α:β. The crude

† Where the $^{13}C$ NMR attached proton test was performed, + signifies a $CH_3$ or CH and − signifies a quaternary carbon or $CH_2$.

product was deprotected using sodium methoxide by the same method as the β anomer **1** and the residue purified by flash column chromatography ($SiO_2$,$CH_2Cl_2$–MeOH, 9:1) to give the glucopyranoside **6** (1.07 g, 74.8%) as needles, mp 118–120 °C; $R_f$ ($SiO_2$, $CH_2Cl_2$–MeOH, 9:1), 0.1; $\nu_{max}/cm^{-1}$ ($CH_2Cl_2$) 3405 (OH) and 1080 (CO); $\delta_H$[400 MHz, $(CD_3)_2SO$] 4.73 [1 H, d, *J* 5.4, CHO*H* (exc.)], 4.61 [1 H, d, *J* 4.9, CHO*H* (exc.)], 4.49 [1 H, d, *J* 6.3, CHO*H* (exc.)], 4.46 (1 H, d, *J* 3.6, OCHO), 4.31 [1 H, t, *J* 6.0, $CH_2OH$ (exc.)], 3.5–3.2 (6 H, m, $OCH_2R$, $CH_2OH$, CHOH and CHO), 3.03 (1 H, ddd, *J* 9.7, 6.2 and 3.6, CHOH), 2.91 (1 H, td, *J* 9.2 and 5.5, CHOH), 1.4–1.3 (2 H, m, $OCH_2CH_2R$), 1.2–1.1 (22 H, m, $OC_2H_4C_{11}H_{22}CH_3$) and 0.72 (3 H, t, *J* 6.8, $CH_3$); $\delta_C$[100 MHz, $(CD_3)_2SO$] 98.6+ (OCHO), 73.4+, 72.8+, 72.1+ (3 × CHOH), 70.4+ (CHO), 66.9− ($OCH_2R$), 61.0− ($CH_2OH$), 31.4−, 29.4−, 29.2−, 29.1−, 29.0−, 28.8−, 25.8−, 22.2− and 14.1+; *m*/*z* 377.3 (40%, $MH^+$) (Found: $MH^+$, 377.292 00. $C_{20}H_{41}O_6$ requires 377.2902).

**Tetradecyl α-D-glucopyranoside 4,6-(phenyl phosphate) 7.** Dry triethylamine (0.8 $cm^3$, 9.1 mmol) was added to a stirred solution of glucopyranoside **6** (1.60 g, 4.2 mmol) in 900 $cm^3$ of dry dichloromethane containing 5 g of 4 Å molecular sieves and the solution was stirred under argon for 1 h. The solution was then cooled to 0 °C and phenyldichlorophosphate (1.03 g, 4.9 mmol) was added and the reaction stirred for another 3 h at room temp. The solution was then filtered and the filtrate was concentrated *in vacuo*. The residue was purified by flash column chromatography ($SiO_2$, EtOAc–toluene, 2:1) to yield the phosphate triester (1.06 g, 48.5%) as a clear oil; $R_f$ ($SiO_2$, EtOAc–toluene, 2:1), 0.4; $\nu_{max}/cm^{-1}$ ($CH_2Cl_2$) 3563 (OH), 1593, 1490 (C=C), 1319 (P=O) and 1205 (PO); $\delta_H$(400 MHz, $CDCl_3$) 7.31 (2 H, t, *J* 7.8, $H_{meta}$), 7.24 (2 H, d, *J* 8.5, $H_{ortho}$), 7.15 (1 H, t, *J* 7.3, $H_{para}$), 4.83 (1 H, d, *J* 3.8, OCHO), 4.32 (1 H, ddd, *J* 23.7, 10.2 and 4.8, $POCH_AH_B$), 4.22 (1 H, t, *J* 10.1, CHOP), 4.15–4.0 (2 H, m, $POCH_AH_B$ and CHO), 3.95 (1 H, t, *J* 9.0, CHOH), 3.7–3.6 [3 H, m, $OCH_AH_BR$ and 2 × CHO*H* (br)], 3.53 (1 H, dd, *J* 9.3 and 3.8, OCHO), 3.44 (1 H, dt, *J* 9.6 and 6.8, $OCH_AH_BR$), 1.7–1.6 (2 H, m, $OCH_2CH_2C_{12}H_{25}$), 1.4–1.2 (22 H, m, $OC_2H_4C_{11}H_{22}CH_3$) and 0.85 (3 H, t, *J* 6.7, $CH_3$); $\delta_C$(100 MHz, $CDCl_3$) 150.0− (1 C, d, *J* 6.7, $C_{ipso}$), 130.0+ (2 $C_{meta}$), 125.5+ ($C_{para}$), 119.7+ (2 C, d, *J* 4.8, $C_{ortho}$), 98.8+ (OCHO), 81.1+ (1 C, d, *J* 6.8, CHOP), 72.0+ (CHOH), 71.3+ (1 C, d, *J* 8.0, CHO), 69.5− (1 C, d, *J* 7.9, $CH_2OP$), 69.3− ($OCH_2R$), 62.3 (1 C, d, *J* 5.7, CHOH), 31.9−, 29.7−, 29.6−, 29.5−, 29.4−, 29.4−, 26.0−, 22.7− and 14.2+; $\delta_P$(100 MHz, $CDCl_3$, H-coupled) −154.0 (1 P, d, *J* 56.8); *m*/*z* 514.3 (65%, $M^+$), 94 (100%, PhOH) (Found: $M^+$, 514.2689. $C_{26}H_{43}PO_8$ requires 514.2695).

**Tetradecyl α-D-glucopyranoside 4,6-(hydrogen phosphate) sodium salt 2.** Aqueous sodium hydroxide (1 M; 5 $cm^3$) was added to a stirred solution of phosphate triester **7** (1.0576 g, 2.1 mmol) in 45 $cm^3$ of THF and the solution stirred for 15 h. The solution was concentrated *in vacuo* to approximately 10 $cm^3$ and neutralized with 1 M HCl. The resulting solution was then lyophilized to yield a white powder which was placed in a Soxhlet extractor and washed with dichloromethane for 48 h to yield the phosphate diester **2** (0.902 g, 95.2%) as white flakes; $\nu_{max}/cm^{-1}$ (Nujol) 3570 (OH), 1310 (P=O); $\delta_H$(400 MHz, $D_2O$) 4.85 (1 H, d, *J* 3.5, OCHO), 4.15–3.40 (8 H, m, $OCH_2R$, $CH_2OP$, CHOP, 2 × CHOH and CHO), 1.7–1.6 (2 H, m, $OCH_2CH_2R$), 1.4–1.2 (22 H, m, $OC_2H_4C_{11}H_{22}CH_3$) and 0.9–0.8 (3 H, m, $CH_3$); $\delta_C$(100 MHz, $D_2O$) 101.8+ (OCHO), 80.8+ (CHOP), 74.0+ (CHOH), 73.6+ (CHO), 71.5− ($OCH_2R$), 69.5− ($CH_2OP$), 66.5+ (CHOH), 34.7−, 32.7−, 32.3−, 31.8−, 28.6−, 25.3− and 16.5+; $\delta_P$(250 MHz, $D_2O$, H-coupled) −143.0 (1 P, d, *J* 41.5); $\delta_P$(250 MHz, $D_2O$, H-decoupled) −143.0; *m*/*z* (+ve FAB) 461.4 (100%, $MH^+$).

### Determination of critical micelle concentration (cmc)

The cmc values for **1** and **2** were determined using a spectrofluorimeter (Perkin-Elmer, UK) monitoring the fluorescence emission intensity of *N*-phenyl-1-naphthylamine ($5 \times 10^{-6}$ M) at a wavelength of 400 nm, on excitation at 340 nm. These measurements were carried out at varying concentrations of **1** and **2** up to 2 mM, under the same buffer conditions as for the MECC experiments. The cmc values of the two surfactants were obtained from a plot of fluorescence intensity *versus* surfactant concentration.

### Determination of the mean aggregation number, *N*

The method outlined by Turro and Yekta[11] was applied, using tris(2,2′-bipyridyl)ruthenium chloride (D) and 9-methylanthracene (Q) as the luminescent donor and quencher, respectively. The Perkin-Elmer spectrofluorimeter was again used for these measurements. The concentration of D was fixed at $7.2 \times 10^{-5}$ M and that of Q was varied between 0 and $10^{-4}$ M. The concentration of **1** and **2** was also kept constant at 40 mM. *N* was determined from the slope of a plot of $\ln(I_O/I)$ *versus* the ratio of the concentration of quencher to that of the surfactant. Again the same buffer conditions were used as in the case of the MECC and cmc measurements.

### Capillary electrophoresis

MECC separations were carried out on a Beckman P/ACE Model 2100 (Beckman, High Wycombe, Bucks, UK). A fused silica capillary, 57 cm (effective length, 50 cm) × 50 μm (i.d.) was used. The separation buffer consisted of 30 mM sodium dihydrogen phosphate, 10 mM boric acid and 40 mM of **1** or **2** adjusted to pH 7.1 using dilute sodium hydroxide. The separation voltage was 15 kV at a temperature of 30 °C. Analytes were injected as aqueous solutions using high pressure and were monitored at a constant wavelength of 254 nm.

### Molecular modelling

Initially 55 monomers (for both the α and β anomers) were arranged in an approximate sphere, with the aliphatic tail methyl carbons forming a core nucleus in van der Waals contact. Simulated annealing was used as the sampling procedure to overcome many of the numerous local minima that will be present on such a highly complex potential energy hypersurface. The simulated annealing methodology has been shown by many workers[12,13] to be an effective tool for this type of problem, therefore only the ensemble details will be reported here. A molecular dynamics annealing strategy was employed utilizing: a temperature of 700 K; a Verlet algorithm with an integration time step of 1 fs; 5 ps of high temperature molecular dynamics equilibration; 50 structures were recorded at 500 fs intervals. Each stored structure was subjected to a full geometry optimization to yield representative structures from which a suitable model was chosen. In the simulation, flat-bottomed harmonic tethers were used to overcome the initial problem of bad contacts and to prevent the micelle from evaporating during the high-temperature simulation. These parameters allowed free movement of the terminal aliphatic methyl groups up to a distance of 8 Å from the arbitrarily defined centre of the micelle. If this distance was exceeded then a harmonic force constant was applied to keep them within the constraint distances.

These simulations were performed using the BIOSYM[14] suite of codes, namely INSIGHTII, DISCOVER3.0 and the cvff forcefield. The lowest energy conformation that resulted from the simulated annealing could be a plausible model for the micelle structure within the constraints of the approximations and it was this structure that the flexible docking studies exploited.

The program DELPHI was used to calculate the Poisson–Boltzmann[15] electrostatic potential for each model of the α and β micelle. This surface was subsequently contoured on to a calculated solvent accessible Connolly surface which enabled subtle differences to be displayed between the two micelle structures.

This paper also reports the docking studies of the representative of the dansyl derivatives, namely dansyl-Phe, onto the

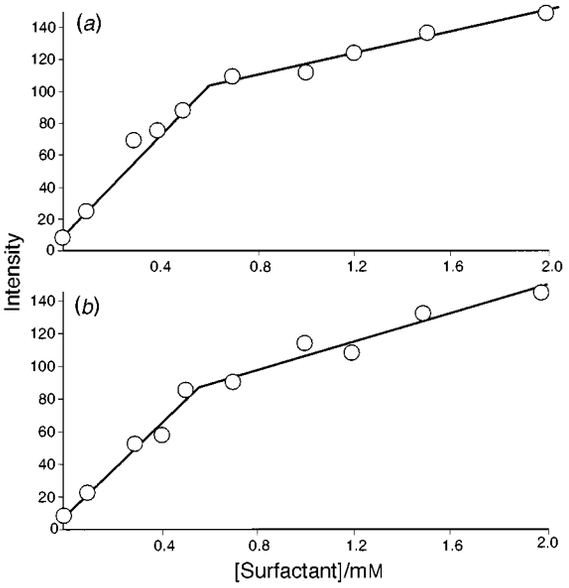


**Fig. 1** Plot of the fluorescence intensity of *N*-phenyl-1-naphthylamine with concentration of (*a*) surfactant **1** and (*b*) surfactant **2**

proposed micelle models. The procedures used to dock the dansyl derivative with the surface of the micelle are again embodied in the BIOSYM software (flexible docking module). This procedure utilizes a Monte Carlo approach, whereby the torsional angles of the dansyl-Phe are perturbed (±180°) and this substrate then replaced at an arbitrary point on the surface (both in Cartesian and angular space). Energy minimisation is subsequently performed on the resulting complex. The interaction energy of the chiral derivative and the micelle surface is calculated and is termed the binding energy; both the minimum and average binding energies are calculated.

### Transmission electron microscopy

Solutions of surfactants **1** and **2** were prepared in 5 mM borate buffer (pH 8.5) at ambient temperature, at two concentrations (4 and 40 mM). Samples were negatively stained on carbon/Formvar coated grids with sodium phosphotungstic acid (pH 7.4) for 15 seconds, blotted dry and examined in a Hitachi H7100 transmission microscope.

## Results and discussion

The fluorescence intensity of the *N*-phenyl-1-naphthylamine is increased substantially as the concentration of **1** or **2** is increased, indicating a high degree of distribution of this hydrophobic probe within micelles [Fig. 1(*a*) and 1(*b*)] formed from either of the two surfactants. This arises due to an increase in the fluorescence quantum yield from the excited probe *via* a reduction of radiationless mechanisms, in particular quenching of the $S^1$ state by molecular oxygen. The break in the plot of the variation of fluorescence intensity with concentration of surfactant indicates the transition from monomeric species to a micellar form. The point of intersection of the two lines for each surfactant gives a measure of the corresponding cmc.

The cmc values for **1** and **2** were found to be virtually identical and were determined as 0.60 and 0.57 mM, respectively. These values are of the same order of magnitude as those determined for two other glucopyranoside surfactants containing an *n*-dodecyl ($C_{12}$) hydrocarbon chain[8] and are more than an order of magnitude lower than that for the commonly used achiral surfactant sodium dodecyl sulfate (SDS).

The measured mean aggregation number (*N*) of **1** and **2** was determined using the method of Turro and Yekta[11] as detailed in the Experimental section. These measurements were carried out using the same buffer conditions as those used in the

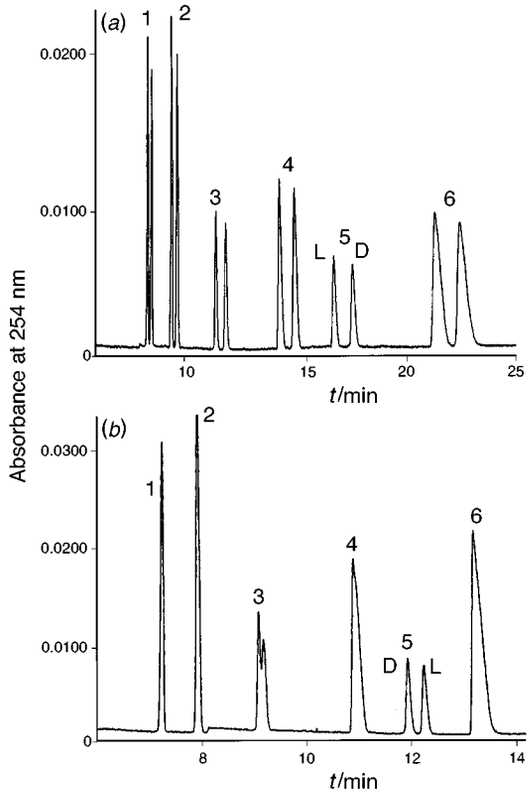


**Fig. 2** Electropherograms showing the separation of the enantiomers of dansylamino acid (DNS) derivatives using (*a*) surfactant **1** and (*b*) surfactant **2**. The numbering of the chiral mixtures shown in this figure refers to the following derivatives: (1) DNS-valine; (2) DNS-norvaline; (3) DNS-leucine; (4) DNS-norleucine; (5) DNS-phenylalanine; (6) DNS-tryptophan.

MECC experiments (see later). Under these conditions *N* was found to be about 65 (±2) for both surfactants. This value is similar to the value of 61 obtained for SDS using either the same method or from membrane osmometry studies.[16,17]

The separation of a mixture of the dansyl derivatives of six amino acid racemates is shown in Fig. 2. From these data it is clear that, under the present conditions of separation, the β-anomer (**1**) is a much superior chiral selector than the α-anomer (**2**). Thus when the former surfactant is included in the separation buffer baseline resolution is obtained for all the dansyl derivatives. In contrast the α-anomer only fully separates the dansyl derivative of phenylalanine.

There is no obvious relationship of migration order to charge density, even though these dansyl derivatives are negatively charged at the pH of this analysis. If this were the case, and assuming that all analytes carry a single negative charge under the conditions of these experiments, then the order of migration should be the reverse of that observed. Under these conditions the 'bulkiest' derivative containing the tryptophan moiety would migrate first as the difference between its electroosmotic and electrophoretic mobilities is the greatest. Conversely, the dansyl derivative with the smaller valine substituent would be expected to migrate last.

In the case of micelles from either **1** or **2** migration times are largely related to the relative hydrophobicity of the dansyl derivatives. Thus the dansyl derivative of valine containing an isopropyl group migrates first and the tryptophan derivative (the most hydrophobic) migrates last. These observations might point to the role played by the surfactant counter-ions (in this case sodium) in the general mechanism of partitioning by micelles. We discuss this further in the context of our molecular modelling studies on **1** and **2** in the following paragraphs.

Comparing Fig. 2(*a*) and 2(*b*) it is also clear that the migration times of the unresolved analytes using **2** are slightly reduced compared to those obtained for the resolved antipodes

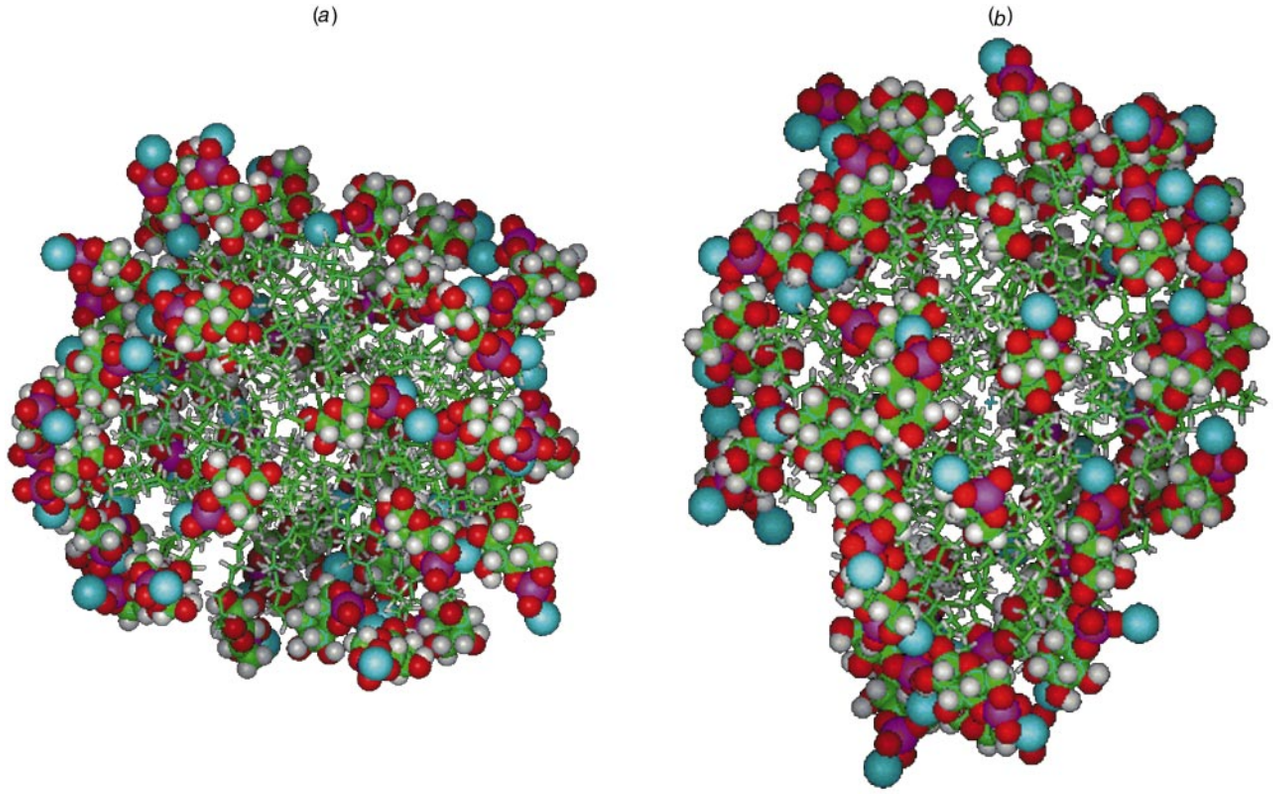


**Fig. 3** Calculated lowest energy structures for micelles formed by (*a*) surfactant **2** and (*b*) surfactant **1**

with surfactant **1**. This behaviour indicates a weaker interaction of the dansyl amino acid derivatives with surfactant **2**.

Not surprisingly, the orientation of the chiral head groups (that is, the glucopyranoside moieties) with respect to each other appears to be the most important feature leading to differences in chiral resolution. It is also interesting that whereas the derivative of the L-amino acid migrates before the corresponding D-enantiomer for all six analytes using **1**, the order of migration for the phenylalanine derivative is reversed when **2** is added to the separation buffer. In the following section we use molecular modelling in an attempt to define the macro- and micro-molecular properties of these micelles, to probe the extent of counter-ion binding, and to explain the observed trends in chiral discrimination.

### Insights from molecular modelling

The lowest energy structures that the simulated annealing procedure evolved are shown in Fig. 3(*a*) and 3(*b*), respectively for both the α- and β-micelles. In this representation, the chiral glucopyranoside head groups are represented as solid spheres (the $Na^+$ counter ions are in cyan) whereas the aliphatic tails are displayed in the stick representation. Both models of the micelle structure clearly display clustering of the chiral head groups. This is due in part to the head group sharing of the $Na^+$ counter-ions. Such a feature would not have been easily predicted without the modelling studies presented here. The calculated radial distribution function of the $Na^+$-oxygen is found to contain a first shell peak at 2.1 Å which is consistent with the $Na^+$ being closely associated with a charged phosphate group. The detailed sub-structure at larger distances is typical of a more fluid-like aspect of the structure, and a detailed inspection of the structure identifies the head group sharing of the counter ions. This phenomenon would be solvent dependent, but the lack of solvent in these simulations is a necessary approximation because of resource constraints. Trends identified *via* isolated/gas phase simulations, are usually observed in solvent simulations: in any case we are concerned primarily with *differences* between two closely similar systems.

There are discrete structural differences between the α- and β-model micelle structures. The β-micelle appears less compact than the α-micelle, the average distance of the phosphorus in the head group from the centre of the micelle being 20.94 Å for the α- and 21.53 Å for the β-micelle. Another interesting structural feature is the amount of solvent-accessible chiral head group surface present for each micelle model. A solvent accessible Connolly surface of the chiral head groups for each micelle reports a value of 7066 $Å^2$ for the α- and 7132 $Å^2$ for the β-micelle. Clearly, if the effectiveness of the micelle is dependent simply on the amount of solvent accessible 'chiral face' then the β-micelle is predicted to be a more effective separation phase than the α.

The surface distribution of electrostatic potential is another property that could enhance the effectiveness of a micelle. Fig. 4 shows the amount of electrostatic potential on the calculated surface for each micelle model. The total charge on the calculated surface has been obtained from these plots: the β-micelles are found to contain more negative potential on the total chiral head group surface as compared to that calculated for the surface on α-micelles.

The above discussion relates to the differences between the predicted structures of the α- and β-micelles, but this does not explain or attempt to model the effective separation of the L- and D-enantiomers of the dansyl derivatives. Thus the separation of one of the dansyl derivatives, dansyl-Phe, was investigated *via* flexible docking of this species onto the surface of each of the isomeric micelles. Although the MECC work reported at this stage of involvement of molecular modelling studies had only investigated the dansyl–β-micelle complex, the interaction with the α-micelle was also investigated *via* computational means. Fig. 5(*a*) and 5(*b*) report the lowest binding energy structure calculated for the interaction of the β-micelle and the L and D stereomers, respectively. Clearly the $Na^+$ counter-ions play an important role in both structures in chelating the carboxylic acid group (which is expected to be deprotonated at the experimental pH of 7.1). The remaining parts of the dansyl derivative interact with another chiral head group. These structural features are interesting since they demonstrate that the chiral *monomer* will be of limited use as a chiral separating

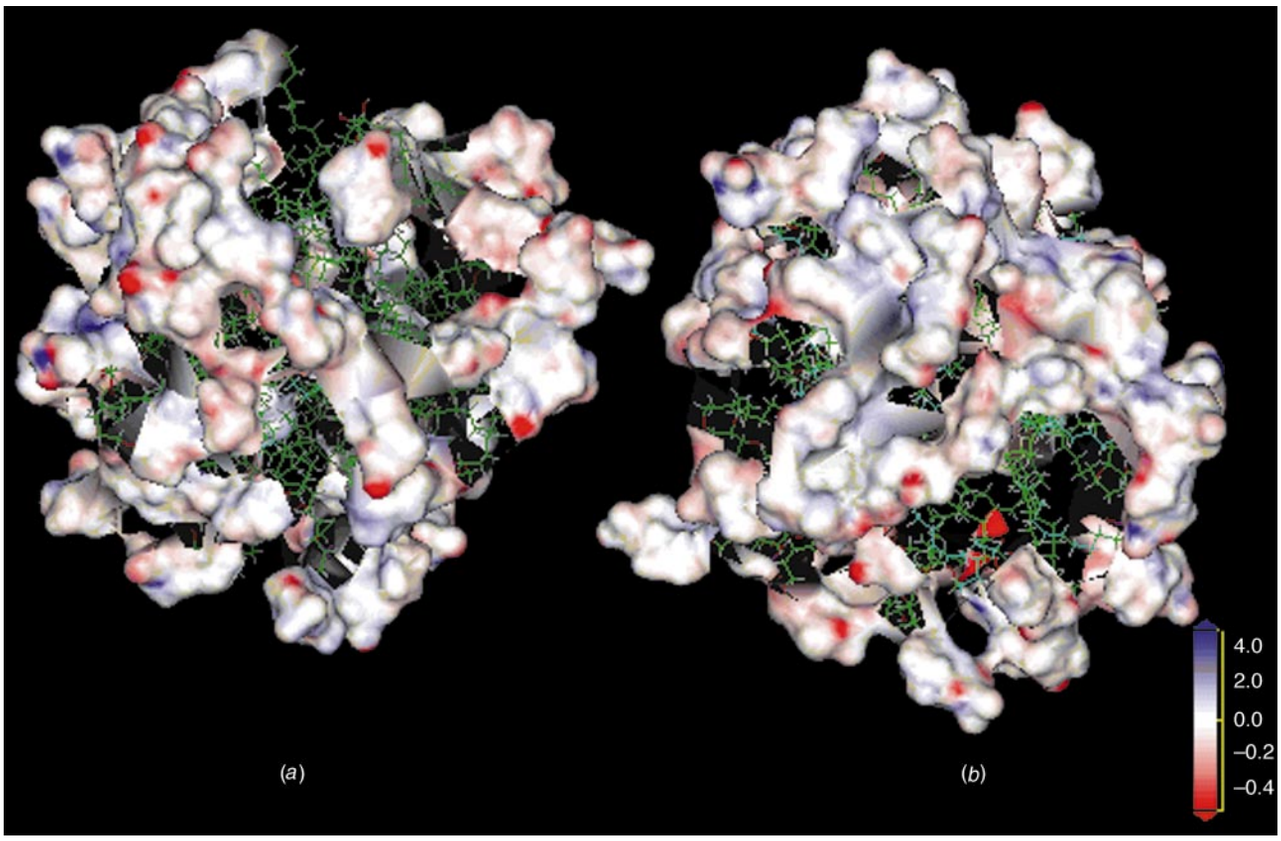


**Fig. 4** Electrostatic potential located on the chiral head groups for (*a*) surfactant **2** and (*b*) surfactant **1**

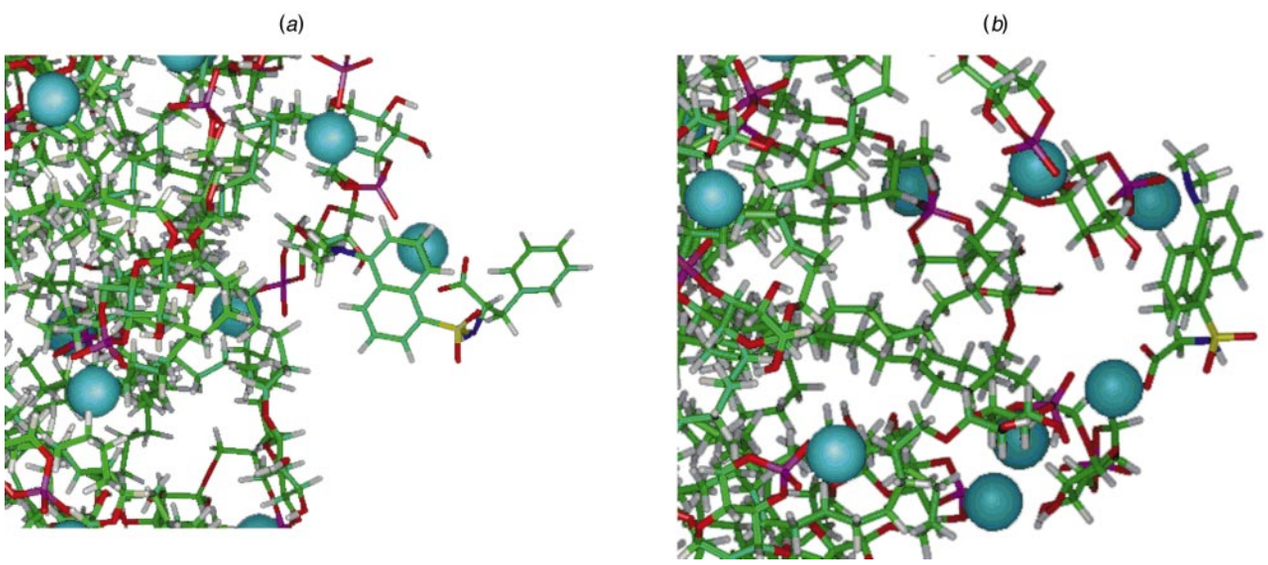


**Fig. 5** Lowest energy structures obtained for (*a*) L-dansylphenylalanine and (*b*) D-dansylphenylalanine interacting with surfactant **1**

agent, since there is not enough 'chiral face' to interact with the dansyl-Phe molecule.

The average and lowest binding energy for these systems can be calculated and these results are displayed in Table 1. Initially focusing on the experimentally known system, the β-dansyl complex, the general trend is that the D-dansyl-Phe binds more tightly to the β micelle than the L-dansyl-Phe, *i.e.* the complex has a lower calculated binding energy. This trend is reproduced for both the calculated lowest binding energy and the average binding energy. Thus on an empirical basis the D form will be retained longer on the micelle, since it has a larger (more negative) binding energy, and hence will elute after the L form. This empirical relationship is in agreement with experimental data.

**Table 1** Calculated binding energies for the interaction of dansyl-Phe and the micelle models

| | α-L | α-D | β-L | β-D |
|---|---|---|---|---|
| Min. binding energy/kcal mol$^{-1}$ | −114.83 | −75.75 | −90.98 | −143.80 |
| Average binding energy/kcal mol$^{-1}$ | −70.29 | −49.30 | −69.40 | −75.84 |

The trend for the dansyl derivative and the β micelle can be reversed for the chiral interactions with the α micelle. These simulations predicted, prior to experiment, that the D form will elute before the L form because for these systems the L form has a larger binding energy than the D form. The experiment has

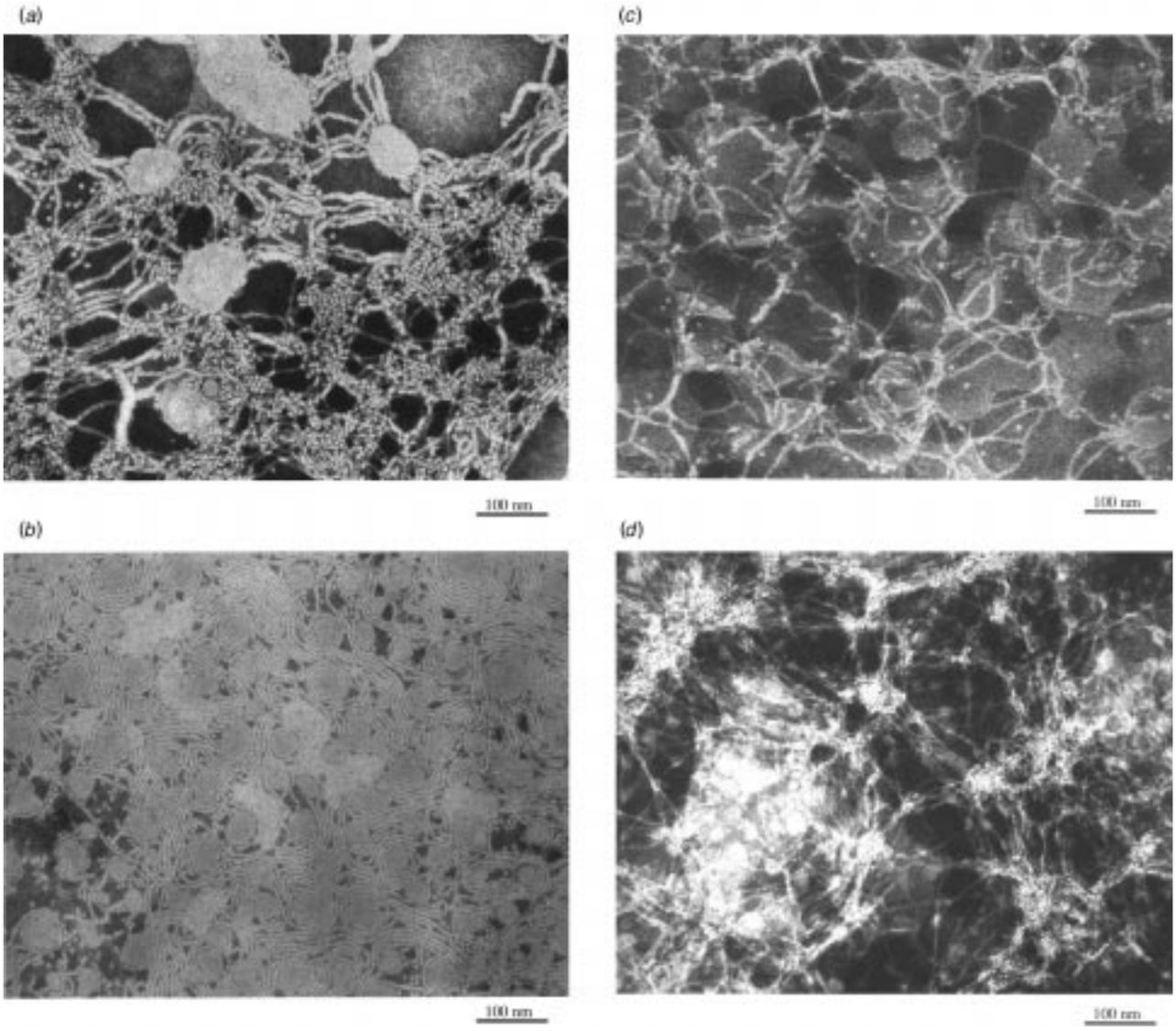


**Fig. 6** Transmission electron microscopy of solutions of surfactant in 5 mM borate buffer: surfactant **1** at (*a*) 4 mM and (*b*) 40 mM; and surfactant **2** at (*c*) 4 mM and (*d*) 40 mM. The length of the scale bars is 100 nm.

since been performed and is in agreement with the prediction: using the α micelle, the D enantiomer elutes before the L form.

**Electron microscopy**

In the present study we have also explored the aggregation behaviour of **1** and **2** using transmission electron microscopy. It should be emphasized that as the samples were air dried in the presence of an electron dense background stain, the organization properties of **1** and **2** may be different from those in free solution. The two surfactants were each studied at 4 and 40 mM concentrations. Results are shown in Fig. 6(*a*)–(*d*). Note that during the preparation of the negative stains surfactant **1** spread the stain more evenly than **2**. At 4 mM concentration, the latter surfactant appeared to be less ordered than **1**; 5–10 nm spherical structures surrounded by a haphazard array of fibrillar/string-like forms were observed for **2**. In contrast, **1** showed aggregates made up of spherical forms that appeared in some instances to coalesce into ordered string-like arrays.

At 40 mM the ordered nature of surfactant **1** was even more apparent. The 5–10 nm spherical forms were reduced in number with extensive developments of the string forms into parallel arrays and whorls. Amongst these structures, foci of larger 25–120 nm droplets were present that might represent a degree of coalescence/nucleation between strings. This level of organization was not evident in **2** where the strings appeared criss-crossed between aggregates of spherical forms of varying size and shape.

## Conclusions

We have shown that the chiral separation efficiency of D-glucopyranoside anionic surfactants depends strongly on the orientation of the $C_{14}$ hydrocarbon chain at the anomeric carbon centre. The order of migration in the analysis of racemic mixtures of dansyl derivatives using these α- and β-surfactants at concentrations above their cmc could be explained by molecular modelling studies. We have also shown by transmission electron microscopy that inversion at the anomeric centre has a marked effect on the extent of organisation of micro-structures formed by the two isomeric surfactants.

## References

1 S. Fanali, *J. Chromatogr.*, 1989, **474**, 441.
2 M. J. Sepaniak, R. O. Cole and B. K. Clark, *J. Liq. Chromatogr.*, 1992, **15**, 1023.
3 T. Ueda, F. Kitamura, R. Mitchell, T. Metcalf, T. Kuwara and A. Nakamoto, *Anal. Chem.*, 1991, **63**, 2979.
4 S. Terabe, M. Shibita and Y. Miyashita, *J. Chromatogr.*, 1989, **480**, 403.

5 R. O. Cole, M. J. Sepaniak and W. L. Hinze, *J. High Resolut. Chromatogr.*, 1990, **13**, 579.
6 G. E. Barker, P. Russo and R. A. Hartwick, *Anal. Chem.*, 1992, **64**, 3024.
7 M. P. Gasper, A. Berthod, U. B. Nair and D. W. Armstrong, *Anal. Chem.*, 1996, **68**, 2514.
8 D. C. Tickle, G. N. Okafo, P. Camilleri, R. F. D. Jones and A. J. Kirby, *Anal. Chem.*, 1994, **66**, 4121.
9 V. de Biasi, J. Senior, J. A. Zukowski, R. C. Haltiwanger, D. E. Eggleston and P. Camilleri, *J. Chem. Soc.*, *Chem. Commun.*, 1995, 1575.
10 M. Bouzige, G. Okafo, D. Dhanak and P. Camilleri, *Chem. Commun.*, 1996, 671.
11 N. J. Turro and A. Yekta, *J. Am. Chem. Soc.*, 1978, **100**, 5951.
12 F. Guarnieri and H. Weinstein, *J. Am. Chem. Soc.*, 1996, **118**, 5580.
13 R. Tejero, D. Bassolinoklimas, R. E. Bruccoleri and G. T. Montelione, *Protein Sci.*, 1996, **5**, 578.
14 BIOSYM, 9625 Scranton Road, San Diego, California, USA.
15 B. Honig, K. Charp and A. J. Yang, *J. Phys. Chem.*, 1993, **97**, 1101.
16 P. Camilleri and G. N. Okafo, *J. Chem. Soc.*, *Chem. Commun.*, 1992, 530.
17 M. F. Emmerson and A. Holtzer, *J. Phys. Chem.*, 1965, **69**, 3718.

*Paper* 7/08418H
*Received* 21*st November* 1997
*Accepted* 17*th December* 1997